JOURNAL OF NATURAL PRODUCTS

pubs.acs.org/jnp

Article

Androsamide, a Cyclic Tetrapeptide from a Marine *Nocardiopsis* sp., Suppresses Motility of Colorectal Cancer Cells

Jihye Lee,[#] Chathurika. D. B. Gamage,[#] Geum Jin Kim, Prima F. Hillman, Chaeyoung Lee, Eun Young Lee, Hyukjae Choi, Hangun Kim,[*] Sang-Jip Nam,[*] and William Fenical[*]

Cite This: https://dx.doi.org/10.1021/acs.jnatprod.0c00815

Read Online

ACCESS | Metrics & More | Article Recommendations | Supporting Information

ABSTRACT: A cyclic tetrapeptide, androsamide (**1**), was isolated from a marine actinomycete of the genus *Nocardiopsis*, strain CNT-189. The planar structure of **1** was assigned by the interpretation of 1D and 2D NMR spectroscopic data. The absolute configurations of constituent amino acids of **1** were determined by application of the Marfey's and advanced Marfey's methods. Androsamide (**1**) strongly suppressed the motility of Caco2 cells caused by epithelial−mesenchymal transition.

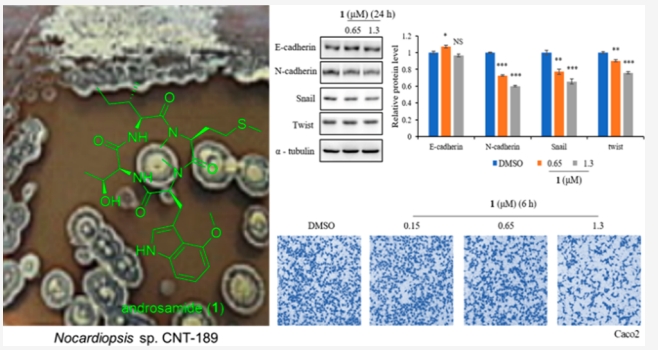

Colorectal cancer (CRC) is the third most deadly diagnosed cancer type and the fourth leading cause of cancer mortality in the world. According to global patterns and trends in CRC incidence and mortality, it is expected to increase by 60% by 2030. More than two-thirds of all CRC incidents and about 60% of all deaths have been recorded in countries with a high or very high human development index (HDI).[1] Metastases are the main cause of mortality in CRC, similar to other malignancies. About 25% of CRC patients were found to have distant metastasis at their initial diagnosis.[2] Human CRC commonly metastasizes to the liver and lungs; more than 50% of CRC patients tend to have liver metastases during their lifespan.[3] Given the severity of this disease, the discovery and development of new diagnostic strategies and new CRC treatments are of urgent need.

Human CRC has many underlying causes. Genetic mutations such as inactivation of tumor suppressor genes or activation of oncogenes, as well as chronic inflammation caused by Crohn's disease or ulcerative colitis, can ultimately lead to CRC occurrence.[4] Epithelial−mesenchymal transition (EMT) is a complicated cellular mechanism in which cells change their epithelial characteristic to acquire migratory and invasive properties. EMT is considered a primary mechanism for CRC progression and metastasis.[5] That is, this phenomenon supports tumor cells' ability to survive against constant changes in the tumor microenvironment and to invade other organs successfully.[6] Some extracellular stimuli, such as inflammatory cytokines, growth factors, or hypoxic conditions generated in the tumor microenvironment, regulate EMT abnormally in cancer cells. Given this situation, inhibition of the EMT process has become one of the most important aims for the development of anticancer therapeutics.

As part of our efforts to discover anticancer agents from natural products, we focused on screening the secondary metabolites produced by the genus *Nocardiopsis*. The genus *Nocardiopsis* has been a prominent marine bacterial source of bioactive metabolites, along with members of the genus *Streptomyces*.[7] *Nocardiopsis* strains have been reported to produce many unique bioactive metabolites, such as cyclic peptides, polyketides, macrolides, chlorinated aromatic compounds, and terpenoids, including lucentamycins A−D,[8] lucentides A and B,[9] borrelidins C−E,[10] fijiolides A and B,[11] and nocarimidazoles A and B.[12] *Nocardiopsis* strain CNT-189, isolated from a Bahamas shore sediment, was investigated to discover new anticancer agents. This strain was first identified as a *Streptomyces* sp. by analysis of a limited range of NCBI Blast data. On re-examination, analysis of 16S rRNA sequence data clearly showed this strain to be a member of the genus *Nocardiopsis*. This bacterial strain has been reported to produce the kromycin aglycones of pikromycin, 4*Z*-, 4*E*-12-deoxydihydrokromycins.[13] In this work, following extensive investigation of the chemical components from the culture broth of strain CNT-189, a new cyclic peptide, androsamide (**1**), was isolated.

Received: July 21, 2020

Herein, we report the isolation, structure elucidation, and bioactivities of **1**.

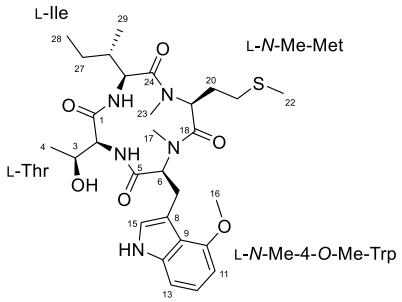

Androsamide (**1**)

RESULTS AND DISCUSSION

Androsamide (**1**) was isolated as a yellowish powder, and its molecular formula was determined to be $C_{29}H_{43}N_5O_6S$ on the basis of (+)-HRESIMS, coupled with analysis of NMR data. The ^{1}H NMR spectrum of **1** showed two exchangeable amide protons (δ_H 6.71 and 7.45), an amine proton (δ_H 10.85), and four α-amino protons (δ_H 3.42, 3.80, 4.29, and 4.64), typical features for a peptide, as well as an oxygenated methine proton (δ_H 3.96), two methyl doublets (δ_H 0.90 and 0.97), two *N*-methyl groups (δ_H 2.29 and 2.93), and one *S*-methyl group (δ_H 1.95). The ^{13}C NMR spectrum displayed 29 carbons, including four amide carbonyls (δ_C 170.2, 170.4, 171.1, and 171.6) and four α-amino carbons (δ_C 52.7, 54.9, 55.2, and 61.8).

Analysis of COSY, HSQC, and HMBC spectra allowed the establishment of four distinct amino acids: a threonine (Thr), an *N*-methyl-4-methoxy-tryptophan (*N*-Me-4-*O*-Me-Trp), an *N*-methyl-methionine (*N*-Me-Met), and an isoleucine (Ile). A Thr unit was defined by COSY NMR data that illustrated cross-peaks from H_3-4 (δ_H 0.97, d, J = 5.0 Hz) to 2-NH (δ_H 7.45, d, J = 8.0 Hz) and by HMBC correlations from 2-NH to C-1 (δ_C 170.4). The COSY correlations from H_3-28 (δ_H 0.82, t, J = 5.8 Hz) to 25-NH (δ_H 6.71, d, J = 7.6 Hz) and from H_3-29 (δ_H 0.90, d, J = 5.4 Hz) to H-26 (δ_H 1.65, m) and HMBC correlations from 25-NH to C-24 (δ_C 171.6) indicated an Ile unit. A Met moiety was assigned by interpretation of COSY cross-peaks from H-19 (δ_H 4.29, m) to H_2-21 (δ_H 2.47, m; 2.35, m) and by HMBC correlations from H_3-22 (δ_H 1.95, s) to C-21 (δ_C 30.1) and from H-19 to C-18 (δ_C 170.2). The HMBC correlation from H_3-23 (δ_H 2.93, s) to C-19 (δ_C 55.2) indicated that an amide proton of the Met residue was replaced with an *N*-methyl group. Lastly, a Trp moiety was identified by the COSY NMR cross-peaks between H-6 (δ_H 3.80, m) and H-7 (δ_H 3.26, d, J = 7.6 Hz) and by HMBC correlations of H-6 and H-7 to C-5 (δ_C 171.1), of H-7 to C-8 (δ_C 110.9) and C-9 (δ_C 116.9), of H-15 (δ_H 6.88, s) to C-8, C-9, and of 14-NH (δ_H 10.85, s) to C-14 (δ_C 138.0) and C-15, along with the ^{1}H−^{1}H coupling of the aromatic protons, H-11 (δ_H 6.44, d, J = 5.6 Hz), H-12 (δ_H 6.94, t, J = 5.6 Hz), and H-13 (δ_H 6.91, d, J = 5.6 Hz), and their HMBC correlations. In addition, HMBC correlations from methoxy protons H_3-16 (δ_H 3.79, s) to C-10 (δ_C 153.9) and from *N*-methyl protons H_3-17 (δ_H 2.29, s) to C-6 (δ_C 64.3) revealed that a Trp moiety was modified as an *N*-Me-4-*O*-Me-Trp (Figure 1).

The sequence of amino acids was established by analyses of key long-range HMBC and ROESY correlations. A Thr was positioned next to Ile by HMBC correlations from H-25 of Ile to C-1 of Thr. The ROESY correlation between amide protons of

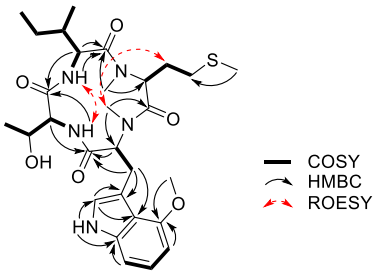

Figure 1. COSY, key HMBC, and ROESY NMR correlations for androsamide (**1**).

Thr and Ile also supported this linkage. The HMBC correlations from H-2 of Thr to C-5 of *N*-Me-4-O-Me-Trp permitted that the modified Trp to be attached next to Thr. The connectivity of *N*-Me-4-*O*-Me-Trp to *N*-Me-Met was identified based on HMBC correlations from H_3-17 to C-18 (δ_C 170.2). This linkage was also confirmed by the ROESY correlation between *N*-methyl protons of the modified Trp and H_2-20 (δ_H 2.08, m, 1.56, m) of *N*-Me-Met. Lastly, HMBC correlation from H_3-23 to C-24 (δ_C 171.6) allowed the connection between *N*-Me-Met and Ile.

The absolute configurations of both Ile and Thr were determined to be L by Marfey's analysis with 1-fluoro-2,4-dinitrophenyl-5-D-leucine amide (D-FDLA) by the comparison of the retention time with authentic standards (Table S1 and Figure S7). The absolute configurations of modified amino acids (*N*-Me-4-O-Me-Trp and *N*-Me-Met) were analyzed by the advanced Marfey's method (Table S2 and Figure S8). The reaction products of *N*-Me-4-*O*-Me-Trp with L-FDLA and D-FDLA were detected at the retention times of 7.6 and 11.5 min, respectively. The derivatives of *N*-Me-Met with L-FDLA and D-FDLA were found at the retention times of 13.3 and 18.7 min, respectively. Therefore, the absolute configurations of both *N*-Me-4-*O*-Me-Trp and *N*-Me-Met were assigned as L configurations.[14]

Modified amino acids in peptides, and particularly those that are *N*-methylated, are extremely important secondary metabolites from ascidians and sponges.[15] The occurrence of an *N*-Me-Met and an *N*-Me-4-*O*-Me-Trp in marine natural products is rare. With regard to *N*-Me-Met, it was found in microginin 674 and microginin 511 produced by the cyanobacterium *Microcystis aeruginosa*.[16] Interestingly, this is the first report of an *N*-Me-4-*O*-Me-tryptophan residue in marine natural products. In the terrestrial environment, the heptadepsipeptide cycloheptamycin A produced by a terrestrial *Streptomyces* sp. is the only example in the literature.[17] Consequently, **1** is unique in containing this rare amino acid.

Compound **1** was tested for its cytotoxicity against a variety of cancer cell lines. Relative cell viability of human gastric adenocarcinoma (AGS), human colorectal adenocarcinoma (Caco2), and human colorectal carcinoma (HCT116) was measured by MTT assay after treatment with various concentrations of **1** for 48 h. Treatment with **1** decreased the viability of AGS, Caco2, and HCT116 cells in a dose-dependent fashion (Figure 2). Compound **1** had IC_{50} values of 13 μM (Caco2), 18 μM (AGS), and 21 μM (HCT116) against the three cell lines, indicating that **1** would not be considered cytotoxic (cytotoxicity = IC_{50} < 10 μM). Treatment with high concentrations of **1** (Caco2: 13 μM, 16 μM and HCT116: 21 μM, 26 μM) induces apoptosis in Caco2 and HCT116 cells (Figure S9).

https://dx.doi.org/10.1021/acs.jnatprod.0c00815
J. Nat. Prod. XXXX, XXX, XXX−XXX

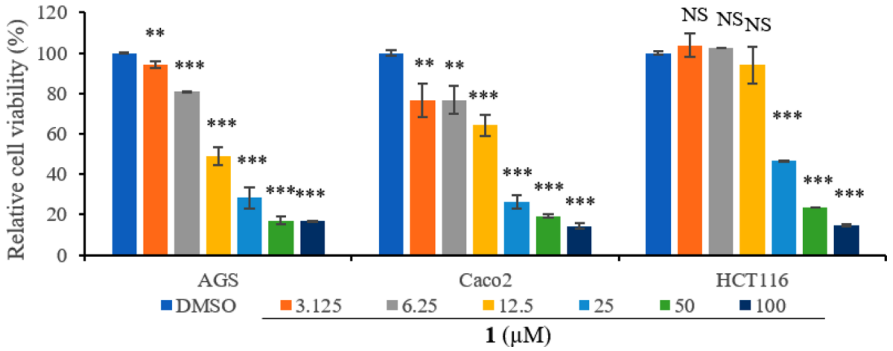

Figure 2. Cytotoxic effects of **1** in Caco2, AGS, and HCT116 cells. Relative cell viabilities of Caco2, AGS, and HCT116 cells were measured by MTT assay, upon treatment with **1** for 48 h at concentrations from 3.125 to 100 μM. Data represent means ± SEM; $n = 3$. *$p < 0.05$; **$p < 0.01$; ***$p < 0.001$; NS, no significant difference compared with the DMSO-treated group.

In order to examine the effect of **1** on Caco2 cell motility at nontoxic concentrations, Transwell migration and invasion assays were performed.[18] Cells were treated with nontoxic concentrations of **1** for 6 h. Compound **1** inhibited Caco2 cell migration in a dose-dependent fashion (Figure 3a). Treatment with 1.3 μM (1/10 of IC_{50}) inhibited the migration by ~50% (Figure 3b). Inhibition of Caco2 cell invasion was assessed after treatment with nontoxic concentrations of **1** for 24 h. A dose-dependent decrement of the number of invaded Caco2 cells was observed upon treatment with **1** (Figure 3c). Approximately 45% of Caco2 cell invasion was inhibited by treatment with 1.3 μM (1/10 of IC_{50}) of **1** (Figure 3d). Taken together, these results indicate that nontoxic concentrations of **1** significantly suppress the motility of Caco2 cells.

Caco2 cells treated with nontoxic concentrations of **1** modulated the expression of EMT markers and downregulated EMT transcription factors. Quantitative real-time PCR (qRT-PCR) assays measured the relative mRNA levels of EMT markers such as E-cadherin, N-cadherin, and vimentin. Treatment with **1** increased E-cadherin level slightly, whereas it decreased N-cadherin and vimentin levels in a dose-dependent fashion (Figure 4a). The levels of EMT transcription factors, Snail, Slug, Twist, ZEB1, and ZEB2, were analyzed after treatment with **1** at nontoxic concentrations for 24 h to determine whether the suppression of Caco2 cell migration and invasion was caused by EMT. mRNA expression of these EMT transcription factors showed significant decrements after treatment (Figure 4b). Moreover, modulation patterns of protein expression of E-cadherin, N-cadherin, Snail, and Twist by Western blotting confirmed the suppression of EMT (Figure 4c). Quantitative analysis of the relative protein level of E-cadherin showed increasing patterns, and N-cadherin, Snail, and Twist showed decreasing patterns similar to relative mRNA levels (Figure 4d). These results suggested that **1** inhibited Caco2 cell motility by regulating EMT. Next, the Human Cell Motility RT^2 Profiler PCR Array was used to examine the expression of cell motility-related genes. Two genes related to human cell motility were screened: calpain 1 (CAPN1) and Ras-related C3 botulinum toxin substrate 2 (RAC2). CAPN1 destabilizes peripheral focal adhesions and increases the rate of membrane detachment, leading to cell migration through a two-dimensional substrate. Also, CAPN1 can cleave numerous substrates to promote cellular motility, such as focal adhesion kinase (FAK), talin paxillin, fodrin, ezrin, vinculin, and α-actinin.[19] RAC2 is responsible for encoding GTP-metabolizing proteins. RAC2 is known to be important in macrophage and endothelial cell migration by regulating vitronectin or fibronectin via $\alpha_v\beta_3$ or $\alpha_4\beta_1$ integrins.[20] Modulation of RAC2 expression has been found in different kinds of human cancers such as brain tumors, head and neck squamous cell cancer, and leukemias.[21] Our results indicate that treatment with **1** decreased the expression of cell motility-related genes CAPN1 and RAC2 in Caco2 cells (Figure 4e). Together, all these findings confirm that **1** is a potential inhibitor against colorectal cancer motility.

EXPERIMENTAL SECTION

General Experimental Procedures. The optical rotation was measured using an Autopol III polarimeter with a 5 cm cell. UV spectra were recorded on a Scinco UVS-2100 spectrophotometer. IR spectra were obtained using a Scimitar 800 FT-IR spectrometer. 1D and 2D NMR spectra were recorded by a Varian Unity-Inova at 400 MHz, using the signals of the residual solvent as internal references (δ_H 2.50 ppm and δ_C 39.52 ppm for DMSO-d_6). High-resolution ESIMS spectra were obtained using a JEOL JMS-AX505WA mass spectrometer. Low-resolution LC-MS data were obtained using an Agilent Technologies 6120 quadrupole LC/MS system with a reversed-phase C18 column (Phenomenex Luna C18 (2), 50 mm × 4.6 mm, 5 μm) at a flow rate of 1.0 mL/min. Column chromatography separation was performed using a C18 column eluting with a gradient of MeOH and H_2O. The fractions were purified using a Waters 1525 binary HPLC pump with a reversed-phase C18 column (Phenomenex Luna C18 (2), 250 mm × 10 mm, 5 μm) eluting with 30% CH_3CN in H_2O at flow rate of 2.0 mL/min.

Strain Isolation. Actinomycete strain CNT-189 was isolated from Bahamas shore sediment from the surf zone. Strain CNT-189 was designated as a *Nocardiopsis* sp. with 99.6% identity by NCBI blast analysis of 16S rRNA gene sequence. The strain CNT-189 DNA sequence was deposited in GenBank (accession number KY111725.1).

Fermentation, Extraction, and Purifircation. Strain CNT-189 was cultured in 40 × 2.5 L Ultra Yield flasks, each containing 1 L of seawater-based medium (10 g starch, 2 g yeast extract, 4 g peptone, 34.75 g artificial sea salt dissolved in distilled H_2O), and shaken at 27 °C at 150 rpm. After 7 days of cultivation, the broth was extracted using EtOAc (40 L overall), and the solvent was removed in vacuo to yield 1.7 g of an EtOAc crude extract. The extract was fractionated using open column chromatography on C-18 resin with a step gradient elution of H_2O and MeOH to yield eight fractions. Fraction 6, eluted with 30% of MeOH in H_2O (226.5 mg), was further separated using an isocratic solvent system of C-18 reversed-phase column chromatography with 50% aqueous CH_3CN to afford six subfractions. The second subfraction (70.3 mg) was purified by reversed-phase HPLC under isocratic conditions with 45% aqueous CH_3CN to yield **1** (13.5 mg).

*Androsamide (**1**):* amorphous, yellowish powder; $[\alpha]^{25}_D$ −10 (*c* 0.75, MeOH); UV (MeOH) λ_{max} (log ε) 200 (2.15), 281 (2.09), and 349 (1.24) nm; IR (KBr) ν_{max} 3295, 2964, 2933, 1668, 1374, 1255, 1081, and 754 cm^{-1}; ^{1}H and ^{13}C NMR data, see Table 1;

https://dx.doi.org/10.1021/acs.jnatprod.0c00815
J. Nat. Prod. XXXX, XXX, XXX−XXX

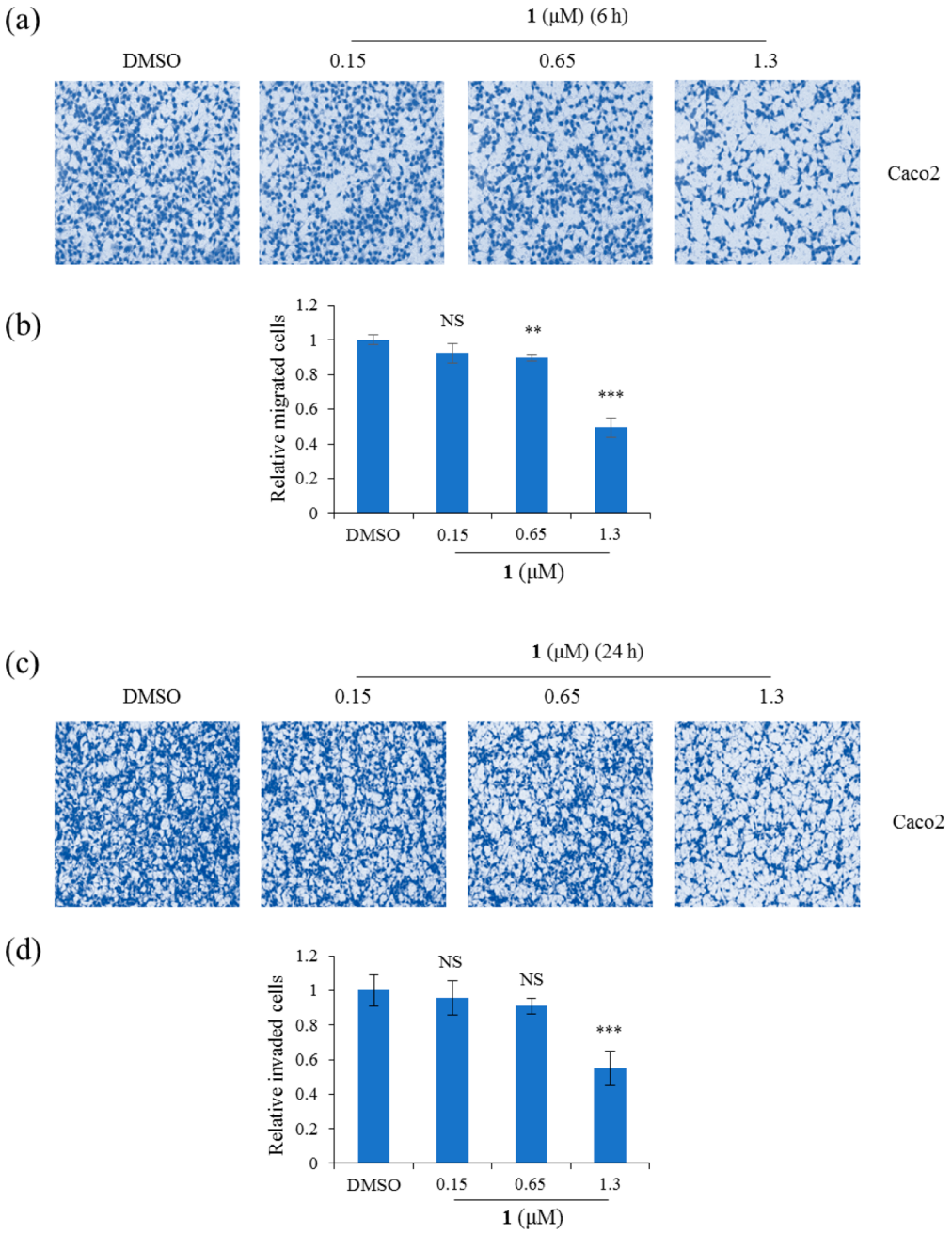

Figure 3. Suppression of Caco2 cell motility by **1**. (a) Representative images of migrated Caco2 cells through the noncoated Transwell after treatment with nontoxic concentrations (0.15, 0.65, 1.3 μM) of **1** for 6 h. (b) Quantitation of relative migrated cells compared to the DMSO-treated control. (c) Representative images of invaded Caco2 cells through the Transwell coated with 1% gelatin after treatment with nontoxic concentrations (0.15, 0.65, 1.3 μM) of **1** for 24 h. (d) Quantitation of relative invaded cells in each treatment group. Data represent means ± SEM; $n = 3$. $^{**}p < 0.01$; $^{***}p < 0.001$; NS, no significant difference compared with the DMSO-treated group.

(+)-HRESIMS, m/z 590.3011 $[M + H]^+$ (calcd for $C_{29}H_{44}N_5O_6S$, 590.3012).

Acid Hydrolysis and Advanced Marfey's Analysis. Compound **1** (100 μg) was hydrolyzed with 100 μL of 6 N HCl at 110 °C for 30 min with stirring. The acid hydrolysate was evaporated under a N_2 gas stream. The dried hydrolysate was resuspended with distilled H_2O and divided into two individual vials. Each reaction vial was dried completely under a N_2 gas stream and in a vacuum freeze dryer. The hydrolysate was dissolved in 100 μL of 1 M $NaHCO_3$. In one vial, the hydrolysate was treated with 25 μL of 1% L-FDLA in acetone. In the second vial, the hydrolysate was treated with 1% D-FDLA in acetone. The reaction mixtures were heated to 50 °C for 30 min with stirring, and the reactions were quenched by addition of 100 μL of 1 N HCl. The reaction products were analyzed by LC-ESIMS with the following chromatographic conditions: Agilent Zorbax SB-C3 column, 5 μm, 150 × 4.6 mm, 50 °C, 1 mL/min, solvent A (0.005% formic acid in H_2O), solvent B (MeOH), A:B = 48:52 → 48:52 (8 min) → 47.5:52.5 (35 min) → 38:62 (55 min) → 0:100 (60 min) → 0:100 (70 min) → 48:52 (72 min) → 48:52 (82 min). The standard amino acids were also prepared and analyzed with the same protocol. All of the reaction products were monitored under UV (340 nm) with a negative ESIMS mode.[13,22]

Cell Culture. The human gastric cancer cell line AGS and the human colorectal cancer cell lines Caco2 and HCT116 were used in these experiments.[23,24] AGS cells were cultured in RPMI, and Caco2 and HCT116 cells were cultured in Dulbecco's modified Eagle medium

https://dx.doi.org/10.1021/acs.jnatprod.0c00815
J. Nat. Prod. XXXX, XXX, XXX−XXX

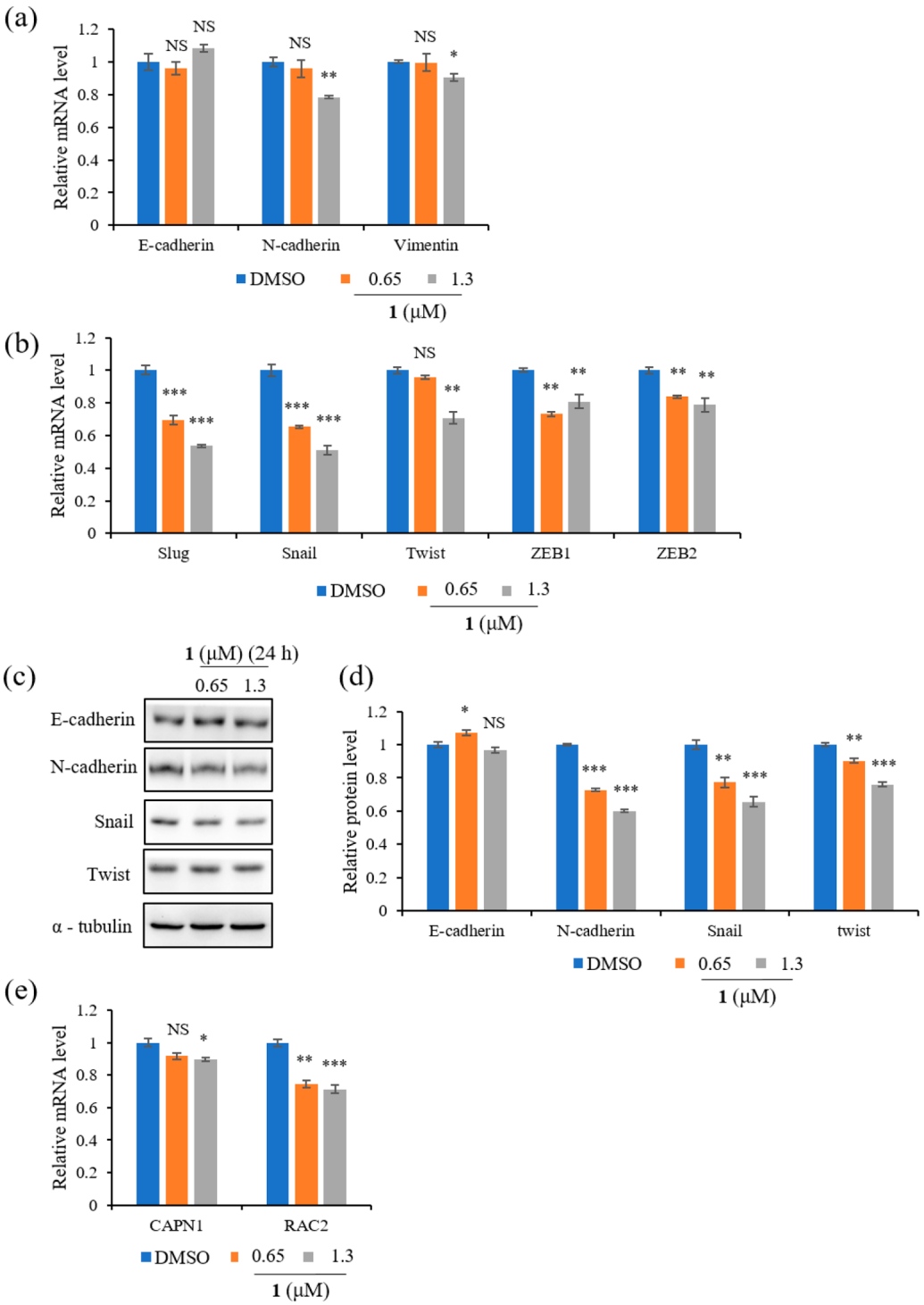

Figure 4. Compound **1** suppressed Caco2 cell motility by suppressing epithelial−mesenchymal transition (EMT) and other motility-related genes. (a) Relative mRNA levels of EMT effectors (N-cadherin, E-cadherin, and vimentin) of Caco2 cells treated with nontoxic concentrations (0.65, 1.3 μM) of **1**. (b) Relative mRNA levels of EMT transcription factors (Slug, Snail, Twist, ZEB1, and ZEB2) of Caco2 cells treated with nontoxic concentrations (0.65, 1.3 μM) of **1**. mRNA levels were normalized against that of GAPDH. (c) Western blotting of E-cadherin, N-cadherin, Snail, Twist, and α-tubulin in cells treated with nontoxic concentrations of **1**. (d) Quantification of relative protein levels of E-cadherin, N-cadherin, Snail, and Twist normalized to the level of α-tubulin, which served as the loading control. (e) Quantitative analysis of the mRNA levels of CAPN1 and RAC2 in Caco2 cells treated with nontoxic concentrations of **1**. Data represent means ± SEM; $n = 3$. *$p < 0.05$; **$p < 0.01$; ***$p < 0.001$; NS, no significant difference compared with the DMSO-treated group.

supplemented with 10% FBS and 1% penicillin and streptomycin. Cells were maintained in an incubator at 37 °C with 5% CO_2. All cell lines were purchased from the Korean Cell Line Bank.

Cell Viability Assay. Viability of AGS, Caco2, and HCT116 cells were measured by the 3-(4,5-dimethylthiazol-2-yl)-2,5-diphenyltetrazolium bromide (MTT) colorimetric assay.[25] Cells were seeded in 96-well plates at a density of $(2-3) \times 10^3$ cells/well and incubated for 12 h. Then cells either were left untreated or were treated with **1** at concentrations ranging from 3.125 to 100 μM and incubated for 48 h followed by incubating with MTT for 4 h. DMSO was added to cells

https://dx.doi.org/10.1021/acs.jnatprod.0c00815
J. Nat. Prod. XXXX, XXX, XXX−XXX

Table 1. ^{1}H and ^{13}C NMR Spectroscopic Data for Androsamide (1) in DMSO-d_6

unit	position	δ_C,[a] type	δ_H, (J in Hz)[b]	COSY	HMBC
Thr	1	170.4, C			
	2	52.7, CH	4.64, dd (8.4, 1.7)	3, 2-NH	5
	3	66.1, CH	3.96, m	2, 4	4
	4	19.8, CH_3	0.97, d (5.0)	3	2, 3
	2-NH		7.45, d (8.0)	2	1, 2
N-Me-4-*O*-Me-Trp	5	171.1, C			
	6	64.3, CH	3.80, m	7	5, 7
	7	25.4, CH_2	3.26, d (7.6)	6	5, 6, 8, 9, 15
	8	110.9, C			
	9	116.9, C			
	10	153.9, C		11	
	11	98.8, CH	6.46, d (5.6)	10, 12	9, 10, 13
	12	121.8, CH	6.95, t (5.6)	10, 13	10
	13	105.0, CH	6.92, d (5.6)	12	9, 14
	14	138.0, C			
	15	122.9, CH	6.88, s		8, 9, 13
	16	54.9, CH_3	3.79, s		10
	14-NH		10.85, s		14, 15
	17-NCH_3	38.6, CH_3	2.29, s		6, 18
N-Me-Met	18	170.2, C			
	19	55.2, CH	4.29, m	20a	18, 21
	20a	25.7 CH_2	2.08, m	19, 20b	21
	20b		1.56, m	21a, 21b	21
	21a	30.1 CH_2	2.47, m	7	
	21b		2.35, m	7	
	22	14.6, CH_3	1.95, s		21
	23-NCH_3	30.6, CH_3	2.93, s		19, 24
Ile	24	171.6, C			
	25	61.8, CH	3.42, t (6.6)	26	1, 24
	26	37.2, CH	1.65, m	25, 27a, 27b, 29	
	27a	24.7 CH_2	1.48, m	26, 27b, 28	
	27b		1.17, m	26, 27a, 28	26, 28, 29
	28	10.8, CH_3	0.82, t (5.8)	27a, 27b	25, 26, 27
	29	15.6, CH_3	0.90, d (5.4)	26	26, 27
	25-NH		6.71, d (7.6)	25	24, 26

[a]Measured at 100 MHz. [b]Measured at 400 MHz.

after removing medium from the wells. Absorbance was measured at 540 nm using a microplate reader and analyzed with Gen 5 (2.03.1) software. Percent relative cell viability was calculated by normalizing the absorbance of cells treated with **1** by that of cells treated with DMSO. IC_{50} was calculated using SPSS statistical software 23.

Flow Cytometric Analysis. Caco2 and HCT116 cells were seeded in six-well plates at a density of (2.0−2.5) × 10^5 cells/well and treated with **1** at cytotoxic concentrations (IC_{50} and 1.25 × IC_{50}) for 6 h.[26] Cells were harvested and washed with ice-cold phosphate-buffered saline followed by adding 100 μL of 1× binding buffer, 6 μL of 50 μg/mL PI, and 3 μL of annexin V−FITC. Cells were incubated in the dark at room temperature for 15 min, and the apoptotic cell population was measured by using a CytoFLEX flow cytometer.

Transwell Migration Assay. Migration of Caco2 cells in response to a chemoattractant was checked using noncoated Boyden chambers (Corning Costar).[27] In total, (2.0−2.5) × 10^5 cells were seeded in each Boyden chamber containing 120 μL of cultural medium with 0.2% bovine serum albumin (BSA). The lower chambers were filled with 400 μL of cultural medium with 0.2% BSA and 10 μg/mL fibronectin (EMD Millipore Corp.) as a chemoattractant. Cells were treated with 0.15, 0.65, and 1.3 μM of **1** and incubated at 37 °C for 6 h. Migrated cells were fixed and stained with a Diff Quick kit (Sysmex) and observed under a K1-Fluo RT fluorescence confocal microscope (Nanoscope Systems). Migrated cells were counted in five random places in each Boyden chamber using iSolution FLAuto software (IMT i-solution Inc.). Experiments were performed in triplicate.

Invasion Assay. Boyden chambers coated with 1% gelatin were used for the invasion assay.[28] Caco2 cells suspended in 100 μL of cultural medium with 0.2% BSA were seeded in each Boyden chamber at a density of 2.5 × 10^6 cells/mL. Lower chambers were filled with 600 μL of cultural medium with 0.2% BSA; 10 μg/mL fibronectin was used as the chemoattractant. Cells were treated with 0.15, 0.65, and 1.3 μM **1** and incubated at 37 °C for 24 h. Invaded cells were fixed and stained with a Diff Quick kit and observed using a Nikon Eclipse 400 fluorescence microscope (Nikon Instech, Co., Ltd.). Invaded cells were counted in five random fields of each Boyden chamber and analyzed by iSolution FLAutosoftware. Three replicates were performed.

Quantitative Real-Time PCR. Briefly, total RNA was isolated from Caco2 cells using RNAiso Plus (TaKaRa) according to the manufacturer's instructions after treatment with nontoxic concentrations of **1** for 24 h.[29] Total RNA (1 μg) from each treated group was converted to cDNA using an M-MLV reverse transcriptase kit (Invitrogen) and SYBR green (Enzynomics). E-Cadherin (forward) 5′-cagaaagttttccaccaaag-3′ and (reverse) 5′-aaatgtgagcaattctgctt-3′; vimentin (forward) 5′-tgccctaaaggaaccaatg-3′ and (reverse) 5′-tccagcagcttcctgtaggt-3′; N-cadherin (forward) 5′-ctcctat gagtggaacag-gaacg-3′ and (reverse) 5′-ttggatcaatgtcataatcaagtgctgta3′; Snail (forward) 5′-tcccgggcaatttaacaatg-3′ and (reverse) 5′-tgggagacacatcggtcga-3′; Slug (forward) 5′-cgaactggacacacatacagtg-3′ and (reverse) 5′-ctgaggatctctggttgtggt-3′; Twist (forward) 5′-cgggagtccgcagtctta-3′ and (reverse) 5′-tgaatcttgctcagcttgtc-3′; ZEB1 (forward) 5′-atgacacagga-aaggaagg-3′ and (reverse) 5′-agcagtgtcttgttgtag-3′; ZEB2 (forward) 5′-caagaggcgcaaacaagcc-3′ and (reverse) 5′-ggttggcaataccgtcatcc-3′; CAPN1 (forward) 5′-gaaggcaacgagttctggag-3′ and (reverse) 5′-ggtccacgttgttccactct-3′; RAC2 (forward) 5′-aagaagctggctcccatcacctac-3′ and (reverse) 5′-aacacggttttcaggcctctctg-3′; GAPDH (forward) 5′-atcaccatcttccagga gcga-3′ and (reverse) 5′-agttgtcatggatgaccttggc-3′ were the primers used in RT-PCR. qRT-PCR reaction and analysis were performed using CFX (Bio-Rad).

Western Blotting. In total, 2 × 10^5 cells per well were seeded in six-well plates and treated with nontoxic concentrations of **1** and incubated for 24 h.[29] Cells were lysed, and the extracted protein was separated using SDS-PAGE. Proteins were detected against primary antibodies E-cadherin, N-cadherin (BD Bioscience), Snail/Slug, Twist (Abcam), and α-tubulin (Cell Signaling Technology). Primary antibodies were detected with horseradish peroxidase-conjugated secondary antibodies (Thermo Fisher Scientific). Band densities were detected under luminescence imaging (iBright FL1000 Imaging System, Thermo Fisher Sciences) and measured by Multi Gauge 3.0. Relative density was calculated against the density of the α-tubulin bands. Values were expressed as arbitrary densitometric units corresponding to signal intensity.

RT^2 Profiler PCR Array. The Human Cell Motility RT^2 Profiler PCR Array (Qiagen, SA Biosciences) was used to examine the expression of cell motility-related genes from Caco2 cells treated with **1**.[27,28] The expression of 84 key genes related to cell motility was profiled according to the manufacturer's instructions. The fold change of mRNA expression was calculated on the basis of the cycle threshold values obtained from the RT-PCR experiment. The scatter plot of test versus control samples indicated the validity of the experiment.

Statistical Analysis. All experiments were performed in triplicates. All statistical analyses were performed using IBM Statistical Package for Social Science (SPSS) version 22. Treatment effects were assessed by one-way ANOVA posthoc analysis. Unless indicated otherwise, a p-value of <0.05 was considered significant.

https://dx.doi.org/10.1021/acs.jnatprod.0c00815
J. Nat. Prod. XXXX, XXX, XXX−XXX

■ ASSOCIATED CONTENT

Supporting Information

The Supporting Information is available free of charge at https://pubs.acs.org/doi/10.1021/acs.jnatprod.0c00815.

^{1}H, ^{13}C, COSY, HSQC, HMBC, and ROESY NMR spectra of **1**; the Marfey's and the advanced Marfey's analysis of **1**; apoptosis assay result of **1** (PDF)

■ AUTHOR INFORMATION

Corresponding Authors

Hangun Kim − *College of Pharmacy, Sunchon National University, Sunchon, Jeonnam 57922, Korea*; Email: hangunkim@sunchon.ac.kr

Sang-Jip Nam − *Department of Chemistry and Nanoscience, Ewha Womans University, Seoul 03760, Korea*; orcid.org/0000-0002-0944-6565; Email: sjnam@ewha.ac.kr

William Fenical − *Center for Marine Biotechnology and Biomedicine, Scripps Institution of Oceanography,, University of California−San Diego, La Jolla, California 92093-0204, United States*; orcid.org/0000-0002-8955-1735; Email: wfenical@ucsd.edu

Authors

Jihye Lee − *Laboratories of Marine New Drugs, REDONE Seoul, Seoul 08594, Korea; Department of Chemistry and Nanoscience, Ewha Womans University, Seoul 03760, Korea*

Chathurika. D. B. Gamage − *College of Pharmacy, Sunchon National University, Sunchon, Jeonnam 57922, Korea*

Geum Jin Kim − *College of Pharmacy and Research Institute of Cell Culture, Yeungnam University, Gyeongsan-si, Gyeongsangbukdo 38541, Korea*

Prima F. Hillman − *Department of Chemistry and Nanoscience, Ewha Womans University, Seoul 03760, Korea*

Chaeyoung Lee − *College of Pharmacy, Ewha Womans University, Seoul 03760, Korea*

Eun Young Lee − *Department of Chemistry and Nanoscience, Ewha Womans University, Seoul 03760, Korea*

Hyukjae Choi − *College of Pharmacy and Research Institute of Cell Culture, Yeungnam University, Gyeongsan-si, Gyeongsangbukdo 38541, Korea*; orcid.org/0000-0002-7707-4767

Complete contact information is available at: https://pubs.acs.org/10.1021/acs.jnatprod.0c00815

Author Contributions

#J. Lee and C. D. B. Gamage contributed equally.

Notes

The authors declare no competing financial interest.

■ ACKNOWLEDGMENTS

This research was funded by Basic Science Research Program through the National Research Foundation of Korea (NRF) of the Ministry of Science, ICT & Future Planning (NRF-2017R1D1A1B03028172) and also supported by a Korea Basic Science Institute (National Research Facilities and Equipment Center) grant funded by the Ministry of Education (2020R 1A 6C 101B194).

■ REFERENCES

(1) Arnold, M.; Sierra, M. S.; Laversanne, M.; Soerjomataram, I.; Jemal, A.; Bray, F. *Gut* **2017**, *664*, 683−691.

(2) Vatandoust, S.; Price, T. J.; Karapetis, C. S. *World J. Gastroenterol.* **2015**, *2141*, 11767−11776.

(3) Misiakos, E. P.; Karidis, N. P.; Kouraklis, G. *World J. Gastroenterol.* **2011**, *1736*, 4067−4075.

(4) Zhu, Q. C.; Gao, R. Y.; Wu, W.; Qin, H. L. *Asian Pac. J. Cancer Prev.* **2013**, *145*, 2689−2698.

(5) Vu, T.; Datta, P. K. *Cancers* **2017**, *9*, 1−22.

(6) Thiery, J. P.; Acloque, H.; Huang, R. Y. J.; Nieto, M. A. *Cell* **2009**, *1395*, 871−890.

(7) Carroll, A. R.; Copp, B. R.; Davis, R. A.; Keyzers, R. A.; Prinsep, M. R. *Nat. Prod. Rep.* **2019**, *36*, 122−173.

(8) Cho, J. Y.; Williams, P. G.; Kwon, H. C.; Jensen, P. R.; Fenical, W. *J. Nat. Prod.* **2007**, *70*, 1321−1328.

(9) Sun, M. W.; Guo, Z. X.; Lu, C. H. *Nat. Prod. Res.* **2016**, *30*, 1036−1041.

(10) Kim, J.; Shin, D.; Kim, S. H.; Park, W.; Shin, Y.; Kim, W. K.; Lee, S. K.; Oh, K. B.; Shin, J.; Oh, D. C. *Mar. Drugs* **2017**, *15*, 166−176.

(11) Nam, S. J.; Gaudencio, S. P.; Kauffman, C. A.; Jensen, P. R.; Kondratyuk, T. P.; Marler, L. E.; Pezzuto, J. M.; Fenical, W. *J. Nat. Prod.* **2010**, *73*, 1080−1086.

(12) Leutou, A. S.; Yang, I.; Kang, H.; Seo, E. K.; Nam, S. J. *J. Nat. Prod.* **2015**, *78*, 2846−2849.

(13) Yang, I.; Yoon, J.; Kim, D.; Hahn, D.; Nam, S. − J.; Fenical, W. *Tetrahedron Lett.* **2017**, *58*, 2322−2324.

(14) Fujii, K.; Shimoya, T.; Ikai, Y.; Oka, H.; Harada, K. I. *Tetrahedron Lett.* **1998**, *39*, 2579−2582.

(15) Garcia, A.; Lenis, L. A.; Jimenez, C.; Debitus, C.; Quinoa, E.; Riguera, R. *Org. Lett.* **2000**, *2*, 2765−2767.

(16) Stewart, A. K.; Ravindra, R.; Van Wagoner, R. M.; Wright, J. L. C *J. Nat. Prod.* **2018**, *81*, 349−355.

(17) Qian, Z.; Antosch, J.; Wiese, J.; Imhoff, J. F.; Fiedler, H. P.; Pöthig, A.; Gulder, T. A. M. *Org. Biomol. Chem.* **2019**, *27*, 6595−6600.

(18) Nguyen, T. T.; Yoon, S.; Yang, Y.; Lee, H. B.; Oh, S.; Jeong, M. H.; Kim, J. J.; Yee, S. T.; Crisan, F.; Moon, C.; Lee, K. Y.; Kim, K. K.; Hur, J. S.; Kim, H. *PLoS One* **2014**, *9*, e111575.

(19) Storr, S. J.; Carragher, N. O.; Frame, M. C.; Parr, T.; Martin, S. G. *Nat. Rev. Cancer* **2011**, *115*, 364−374.

(20) Joshi, S.; Singh, A. R.; Zulcic, M.; Bao, L.; Messer, K.; Ideker, T.; Dutkowski, J.; Durden, D. L. *PLoS One* **2014**, *9*, e95893.

(21) Wertheimer, E.; Gutierrez-Uzquiza, A.; Rosemblit, C.; Lopez-Haber, C.; Sosa, M. S.; Kazanietz, M. G. *Cell. Signal.* **2012**, *24*, 353−362.

(22) Vijayasarathy, S.; Prasad, P.; Fremlin, L. J.; Ratnayake, R.; Salim, A. A.; Khalil, Z.; Capon, R. J. *J. Nat. Prod.* **2016**, *79*, 421−427.

(23) Yang, Y.; Bae, W. K.; Nam, S. J.; Jeong, M. H.; Zhou, R.; Park, S. Y.; Tas, I.; Hwang, Y. H.; Park, M. S.; Chung, I. J.; Kim, K. K.; Hur, J. S.; Kim, H. *Phytomedicine* **2018**, *40*, 106−115.

(24) Yang, Y.; Bae, W. K.; Lee, J. Y.; Choi, Y. J.; Lee, K. H.; Park, M. S.; Yu, Y. H.; Park, S. Y.; Zhou, R.; Tas, I.; Gamage, C.; Paik, M. J.; Lee, J. H.; Chung, I. J.; Kim, K. K.; Hur, J. S.; Kim, S. K.; Ha, H. H.; Kim, H. *Sci. Rep.* **2018**, *8*, 16234−16244.

(25) Gamage, C. D. B.; Park, S. Y.; Yang, Y.; Zhou, R.; Tas, I.; Bae, W. K.; Kim, K. K.; Shim, J. H.; Kim, E.; Yoon, G.; Kim, H. *Int. J. Mol. Sci.* **2019**, *20*, 2612−2627.

(26) Yang, Y.; Zhou, R.; Park, S. Y.; Back, K.; Bae, W. K.; Kim, K. K.; Kim, H. *Molecules* **2017**, *22*, 453−460.

(27) Zhou, R.; Yang, Y.; Park, S. Y.; Nguyen, T. T.; Seo, Y. W.; Lee, K. H.; Lee, J. H.; Kim, K. K.; Hur, J. S.; Kim, H. *Sci. Rep.* **2017**, *7*, 8136−8148.

(28) Tas, I.; Han, J.; Park, S. Y.; Yang, Y.; Zhou, R.; Gamage, C. D. B.; Van Nguyen, T.; Lee, J. Y.; Choi, Y. J.; Yu, Y. H.; Moon, K. S.; Kim, K. K.; Ha, H. H.; Kim, S. K.; Hur, J. S.; Kim, H. *Phytomedicine* **2019**, *56*, 10−20.

(29) Yang, Y.; Nguyen, T. T.; Pereira, I.; Hur, J. S.; Kim, H. *Biomolecules* **2019**, *9*, 797−809.